



**Neutronics Optimization Studies for a
Proliferation Resistant Fuel Assembly from the
Fusion-Fission Fuel Factory, SOLASE-H**

M.Z. Youssef, R.W. Conn, and G.A. Moses

October 1978

UWFDM-263

***FUSION TECHNOLOGY INSTITUTE
UNIVERSITY OF WISCONSIN
MADISON WISCONSIN***

**Neutronics Optimization Studies for a
Proliferation Resistant Fuel Assembly from the
Fusion-Fission Fuel Factory, SOLASE-H**

M.Z. Youssef, R.W. Conn, and G.A. Moses

Fusion Technology Institute
University of Wisconsin
1500 Engineering Drive
Madison, WI 53706

<http://fti.neep.wisc.edu>

October 1978

UWFDM-263

"LEGAL NOTICE"

"This work was prepared by the University of Wisconsin as an account of work sponsored by the Electric Power Research Institute, Inc. ("EPRI"). Neither EPRI, members of EPRI, the University of Wisconsin, nor any person acting on behalf of either:

"a. Makes any warranty or representation, express or implied, with respect to the accuracy, completeness, or usefulness of the information contained in this report, or that the use of any information, apparatus, method, or process disclosed in this report may not infringe privately owned rights; or

"b. Assumes any liabilities with respect to the use of, or for damages resulting from the use of, any information, apparatus, method or process disclosed in this report."

NEUTRONICS OPTIMIZATION STUDIES FOR A
PROLIFERATION RESISTANT FUEL ASSEMBLY
FROM THE FUSION-FISSION FUEL FACTORY,
SOLASE-H

M.Z. Youssef
R.W. Conn
G.A. Moses

October 1978

Fusion Research Program
Nuclear Engineering Department
University of Wisconsin
Madison WI 53706 U.S.A.

UWFD-263

Table of Contents

	<u>Page</u>
Figure Captions	ii
List of Tables	ii
I. Introduction	1
II. Proliferation Considerations	1
III. SOLASE-H as a Fissile Fuel Factory	3
IV. Neutronics Optmization Studies	5
IV-1. Blanket Configuration and Calculational Method	15
IV-2. Beryllium as the Neutron Multiplier	11
IV-3. Lead as the Neutron Multiplier	19
IV-4. Optimization Criteria	24
V. Conclusions	25
VI. References	27

Figure Captions

- Figure 1 Side and Top Views of the Radial and the Axial Blankets of SOLASE-H.
- Figure 2 Schematic Representation in Spherical Geometry of the Hybrid Blanket.
- Figure 3 The Fuel Assembly and the Fuel Pin.
- Figure 4 Neutron Sources and Sinks as Function of Be Front Zone Thickness.
- Figure 5 Tritium and U-233 Breeding Rates as Function of Be Front Zone Thickness Per D-T Neutron.
- Figure 6 U-233 Breeding Distribution in Fuel Zone Per D-T Neutron With Be as Front Zone.
- Figure 7 The Reaction Rates Per D-T Neutron vs. Pb Front Zone Thickness.
- Figure 8 U-233 Breeding Rate Distribution in Fuel Zone Per D-T Neutron With Pb as the Front Zone Neutron Multiplier.
- Figure 9 U-233 Breeding Rate Distribution Through 1/2 of the Fuel Zone After Rotation.

List of Tables

- Table 1 Energy Boundaries for the 25-Neutron Energy Groups.
- Table 2 Neutronic Results for Different Blankets.
- Table 3 Reaction Rates of Blanket #6, #4 and #7 Per D-T Neutron.
- Table 4 Reaction Rates of Blanket #9, #10, #10', #11, #12, and #13 Per D-T Neutron.

I. Introduction

Utilizing the energetic D-T neutrons produced in a fusion-fission hybrid reactor to breed fissile fuel (U-233 or Pu-239) by neutron capture in a fertile fuel (Th-232 or U-238) for subsequent use in fission reactors has recently been addressed by several researchers in a variety of fusion systems (i.e., tokamak,⁽¹⁻³⁾ electron beam fusion,⁽⁴⁾ mirror fusion,⁽⁵⁻⁶⁾ laser fusion⁽⁷⁾). The artificially produced fuel will substantially extend the world's fissile fuel reserves.⁽⁸⁾ This will eliminate the increasing threatening shortage in U-235, which represents the only naturally occurring isotope.

The attractiveness of such reactors is due to the two revenue sources that can be obtained, namely, fissile fuel and electric power. In hybrid designs which emphasize a high fissile fuel production rate, fissioning of the bred fuel is minimized in the hybrid blanket and an energy multiplication factor of the order 5 to 20 is attainable.⁽⁹⁾ As an electricity producer, the fissile fuel is burned "in situ" in the hybrid blanket resulting in a high energy multiplication factor, typically 10-40.⁽⁹⁾ Due to energy multiplication, a relaxation in the fusion energy requirements is possible and may lead to early introduction.

in

II. Proliferation Considerations

The linkage between a hybrid reactor as a fissile fuel factory and the fission reactors as fuel burners should meet the safeguard requirements to prevent the diversion and theft of weapon-grade materials and to offer tight proliferation control. Eliminating the re-

processing as an intermediate stage in the coupling between fission reactors and hybrid reactors can render the bred fuel proliferation resistant. However this will be at the full utilization of the fertile fuel. Typical fission reactor fuel assemblies can be placed in a hybrid blanket to enrich the fuel to the proper fissile concentration and render it proliferation resistant by making the fuel cladding highly radioactive. These fuel assemblies, after reaching 3-4% enrichment, are extracted from the hybrid blanket and shipped to the fission reactors for direct use. The spent fuel assemblies from the fission burners are either stored or, if feasible, reinserted in the hybrid blanket for further enrichment. As argued by Feiveson and Taylor,⁽¹⁰⁻¹¹⁾ and discussed by Bethe⁽¹²⁾, spent or highly radioactive fuel bundles should be self-protecting. Should the reprocessing of the spent fuel extracted from the fission reactors be allowed, the fission products and activities can be separated from the fissile and fertile fuel and fresh or partially enriched fuel assemblies can be refabricated and reinserted into the hybrid blanket to close the fuel cycle. The reprocessing plant and the hybrid reactor can be an integrated part of an internationally controlled, physically secure fuel production and reprocessing site which can provide fissile fuel needs to many national convertor reactors.^(8,13)

III. SOLASE-H as a Fissile Fuel Factory

In this report we represent the results of one-dimensional optimization studies of the laser-driven fusion-fission hybrid reactor, SOLASE-H. These studies are aimed at searching for a blanket configuration which results in minimum nonuniformity in the spacial distribution of the bred U-233 from neutron capture in Th-232. A figure-of-merit that maximizes the bred fissile fuel subject to minimizing the peak-to-average enrichment determines the optimum blanket design.

Fig. 1 shows the final design of the SOLASE-H hybrid reactor. This design is based on the optimum blanket obtained in the present study. Th-232 in the form of oxide fuel is used to breed U-233. The reactor cavity is a right circular cylinder surrounding the point fusion source located at the center. The top and bottom blankets are devoted to breeding tritium and comprise 30% of the solid angle subtended at the cavity center. The radius of the cavity is 6 m and the height is 12 m. The ThO₂ fuel assemblies are located only in the radial blanket which allows for 3 assemblies to be stacked on the top of one another. The blanket structure is Zircaloy-2 to be compatible with the cladding of the fuel elements. Sodium is used as a coolant. The front zone of the blanket are pins of lead clad in zircaloy. It has been established in the present study that a Pb front zone leads to a more uniform fissile fuel profile across the fuel assemblies and comparable neutron multiplication when compared to using a Be multiplier. The operating parameters of SOLASE-H are given in Ref. (13,14).

The performance with time of the optimized blanket has been evaluated to establish a rotation scheme for the fuel assemblies which will result in a symmetric fissile fuel distribution across the fuel assemblies when 4% enrichment is reached. The results of these calculations are presented in a companion report. (15)

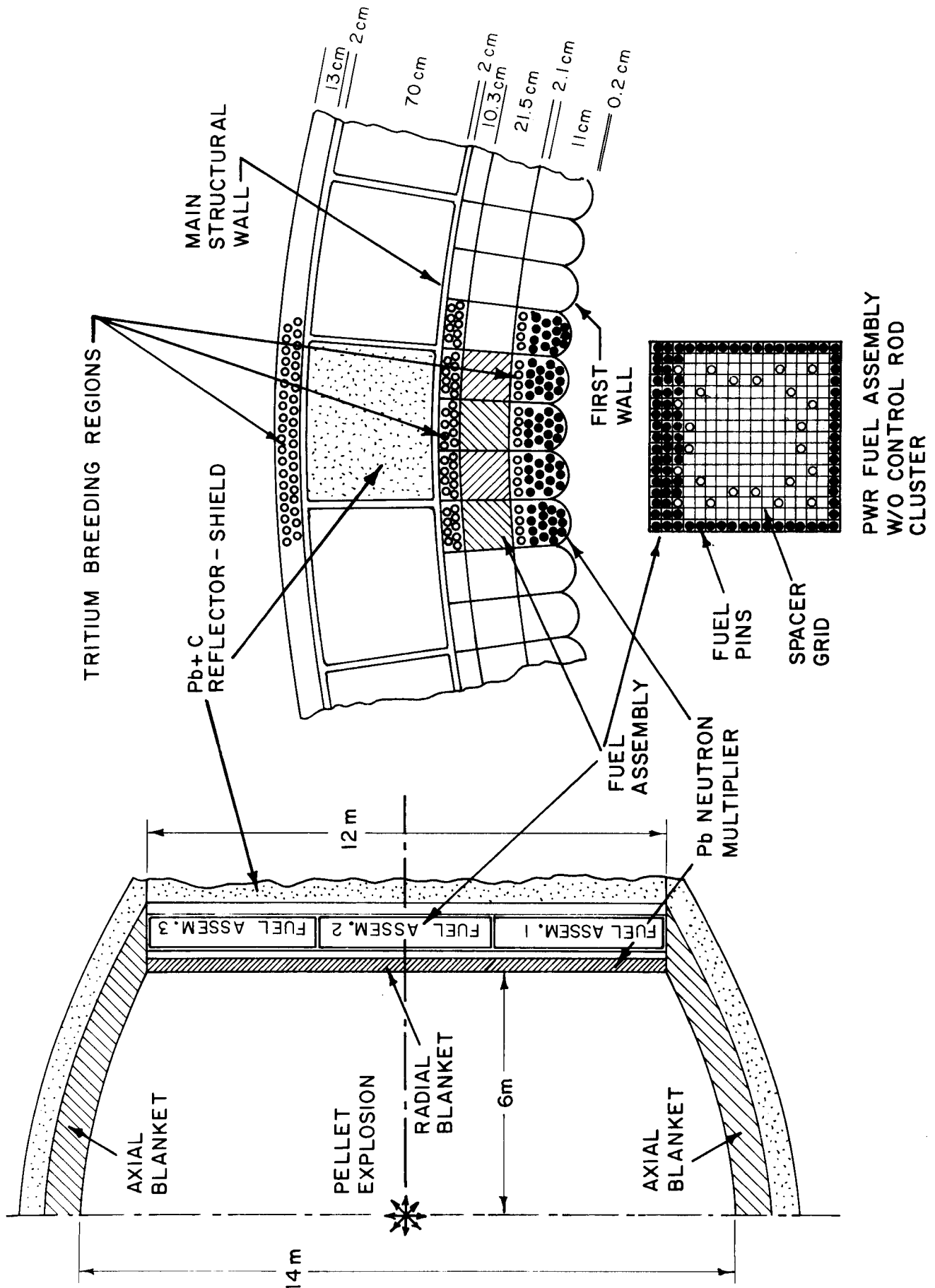


Fig. 1

IV. Neutronics Optimization Studies

The primary objective of the neutronics study reported here has been to maximize the fissile fuel production rate in a hybrid reactor subject to the constraints that the fissile fuel distribution in the fuel zone be as uniform as possible and that the tritium breeding ratio (TBR) be at least 1. We have primarily considered hybrids which produce uranium-233 from thorium because U-233 is a better performing fuel in LWR's, particularly PWR's. However, similar studies can be done on the production of plutonium-239. The constraint of a uniform U-233 distribution throughout the fuel assembly used in the fuel zone is aimed primarily at minimizing the hot spot factor one would calculate for the enriched fuel assembly loaded into a LWR.

IV-1. The Blanket Configuration and Calculational Method

Spherical geometry, one-dimensional calculations have been performed to assess the effects of parameter and design variations and to search for optimum blanket performance. In this regard, two main blanket configurations shown in Fig. 2 have been studied. The first blanket series utilizes beryllium as a neutron multiplier front zone while lead is used in the second series. Lead and beryllium enhance the neutron generation throughout the blanket and replace a U-238 fast fission plate utilized in other studies.⁽¹⁶⁻²⁰⁾ In addition to introducing plutonium into a U-233 fuel cycle, the fission plate would also increase the thermal power generated in the blanket. This would yield excess electricity which could be sold to reduce the overall plant running cost. However, the power increase with time

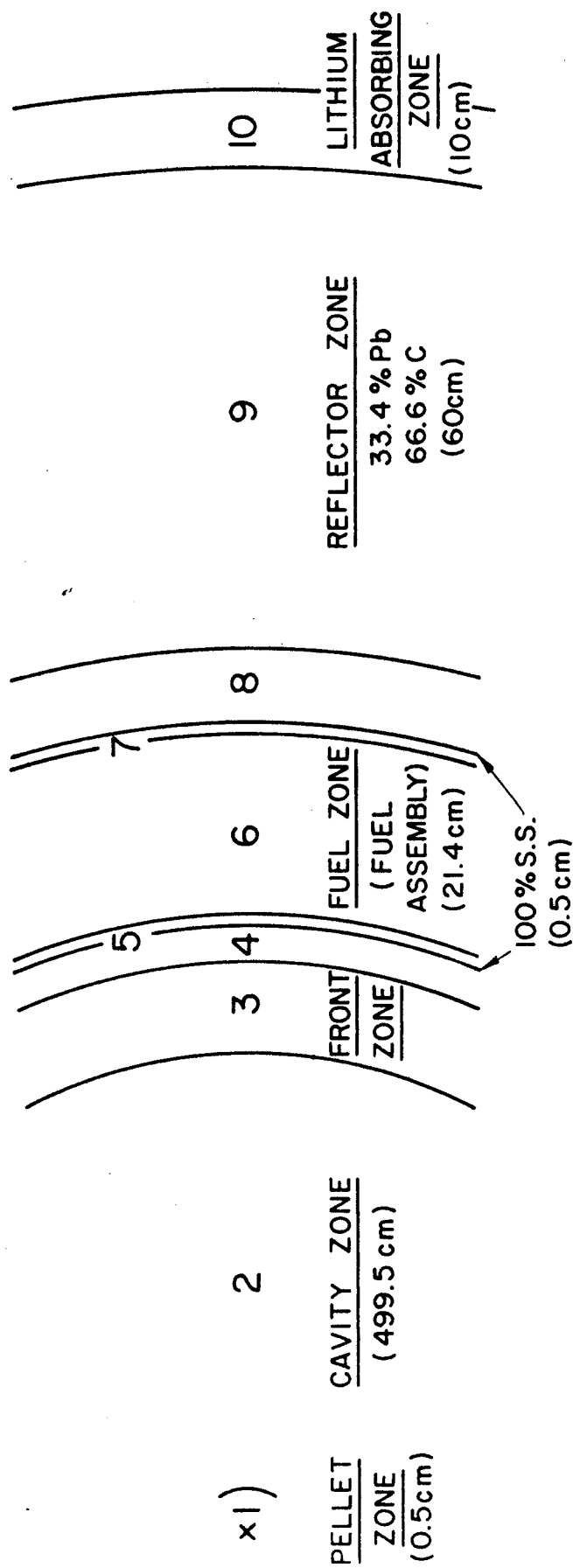


FIGURE 2

SCHEMATIC REPRESENTATION IN SPHERICAL GEOMETRY OF THE HYBRID BLANKET

ZONES 4 AND 8 ARE NOT INCLUDED IN THE SERIES OF
BLANKETS USING Be AS FRONT ZONE MULTIPLIER

makes the design of the cooling system more difficult. In our design, the main concern has been to maximize U-233 production subject to the constraints on fuel production and tritium breeding already mentioned and to ensure sufficient power to make the plant at least self-sufficient in power.

For both classes of reactor blankets (beryllium or lead as a neutron multiplier), the U-233 breeding zone (fuel zone) consists of just one fuel assembly row located behind the neutron multiplier zone. A reflector is positioned behind the fuel zone and consists of 1/3 Pb and 2/3 graphite by volume. The thickness of this reflector is held at 60 cm in all cases. A final liquid lithium neutron absorbing region is located at the outer portion of the blanket.

The fuel zone is thus located in a flux trap between the reflector and the neutron multiplying zone. For this reason, two relatively thin neutron absorbing lithium zones are located immediately in front of and behind the fuel assembly zone in the series of blankets utilizing lead as front zone neutron multiplier. This achieves two ends: 1. Thermal neutrons which would be absorbed at the edge of the fuel assembly are filtered out. Thus, only harder neutrons penetrate and this produces a more uniform U-233 production rate. 2. The neutrons absorbed in the lithium help to meet the constraint that the tritium breeding ratio be 1.

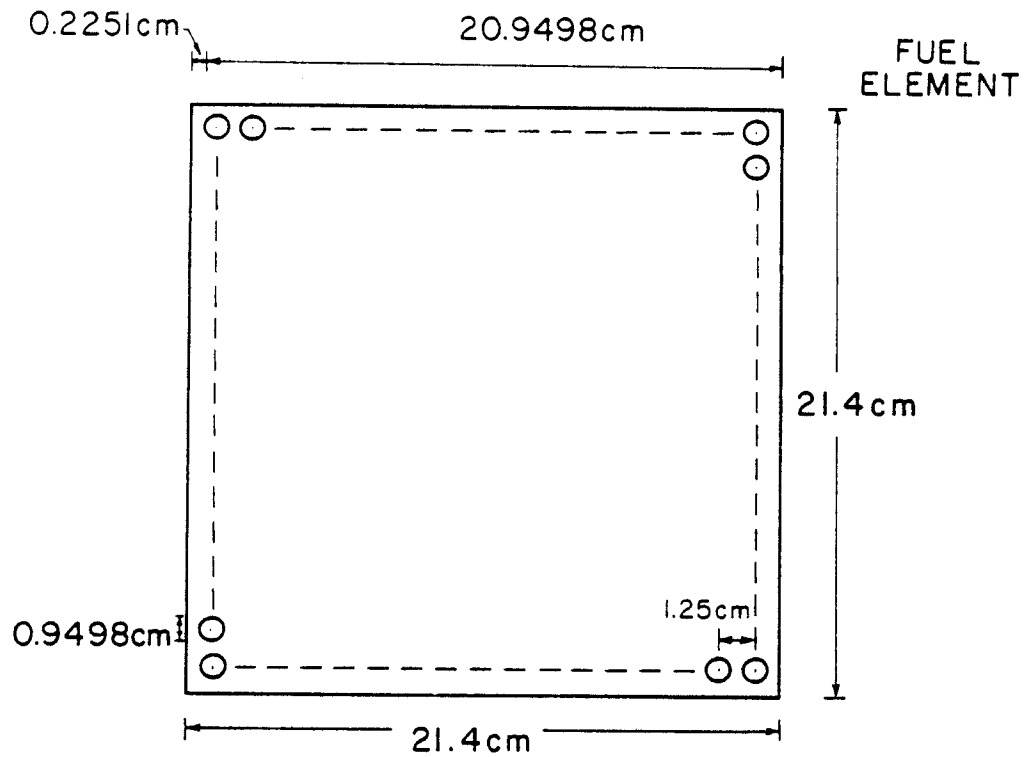
A square single PWR assembly has 264 fuel elements arranged in a 17 x 17 array and is 21.4 cm on a side. The fuel pins have an outer diameter of 0.9498 cm and a square pitch of 1.25 cm. Zircaloy-2 is utilized as the cladding material with a thickness of 0.0572 cm. The ThO_2 fuel pellet diameter is 0.819 cm. Each fuel assembly contains 25 empty locations of outer diameter 0.9498 cm and are reserved for the control rods when the

fuel assembly is extracted from the blanket and used in LWRs. The dimensions of the fuel assembly and the fuel pins are shown in Fig. 3. The fuel assembly used in this study is typical of those used in a PWR.⁽²⁴⁾ The volume percentages corresponding to the dimensions shown in Fig. 3. are: 30.3% ThO_2 , 9.2% Zircaloy-2, 1.3% void and 59.2% coolant. When the fuel assembly is placed in the blanket, the fuel zone will occupy a region 21.4 cm thick. This is held constant for the blankets studied.

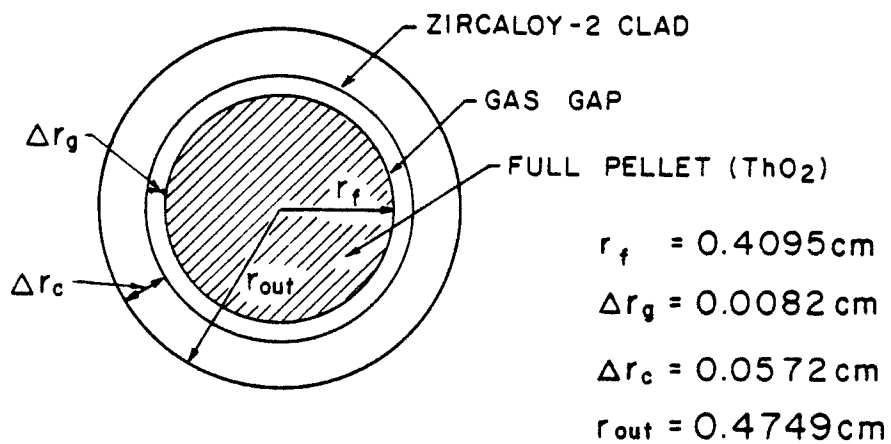
To simulate a laser fusion hybrid, the neutron source is localized in a zone 0.5 cm radius at the center of the reactor. The first wall is at a radius of 5 m in the survey calculations. However, in the final design, the optimized blanket is reconfigured to closely approximate the engineering features and the cylindrical geometry of the actual hybrid concept shown in Fig. 1. As mentioned before, the pellet in that design is centered at 6 m from the first wall and the cylindrical radial blanket section is 12 m high. The top and bottom axial caps are designed to produce tritium. Since the caps are devoted solely to tritium production, one requires less tritium breeding in the radial section. As such, we have used a value of 0.6 as the constraint on TBR in these spherical geometry parametric calculations. This corresponds to a value of ~ 0.4 if 70% of the solid angle subtended by the radial blanket, is considered.

All the neutronic calculations were carried out using the one-dimensional discrete ordinate neutron transport code ANISN. A 25 neutron energy group cross section library has been used based on the DLC-2D⁽²²⁾ library which was generated from ENDF/B III with the SUPERTOG⁽²³⁾ code using a 1/E weighting spectrum for the GAM-II 100-group structure. The energy boundaries for the 25 groups are given in Table 1.

Figure 2 shows the different zones of the blanket for both series mentioned earlier. Zones 4 and 8 are not included in the Be front zone series.



(a) THE 17X17 FUEL ASSEMBLY ;
264 FUEL ELEMENTS AND 25
LOCATIONS FOR CONTROL ROD (TOTAL 289)



(b) FUEL ELEMENT PIN

Fig. 3 THE FUEL ASSEMBLY AND THE FUEL PIN

Table 1 Energy Boundaries for the 25-Neutron
Energy Groups

Group	Energy End Boundaries (eV)	Group	Energy End Boundaries (eV)
1	1.4918 + 07 → 1.3499 + 07	14	2.4660 + 06
2	1.2214 + 07	15	1.3534 + 06
3	1.1052 + 07	16	7.4274 + 05
4	1.0000 + 07	17	4.0762 + 05
5	9.0494 + 06	18	1.6573 + 05
6	8.1873 + 06	19	3.1878 + 04
7	7.4082 + 06	20	3.3546 + 03
8	6.7032 + 06	21	3.5358 + 02
9	6.0653 + 06	22	3.7267 + 01
10	5.4881 + 06	23	3.9279 + 00
11	4.4933 + 06	24	4.1399 - 01
12	3.6788 + 06	25	2.2200 - 02
13	3.0119 + 06		

The constituents and the volume percentages in the different zones of the large number of cases studied are summarized on Table 2. We also give the results for the U-233 breeding ratio UBR (U-233 atoms produced per D-T neutron) and the tritium breeding ratio TBR. Note that cases with Li cooling and Na cooling have been also considered in this parametric study.

IV-2. Beryllium as the Neutron Multiplier

Several different blankets utilizing Be as front zone material were studied. Zircaloy-2 is chosen as the structural material for this zone. The volume percentages are: 82.2%-Be, 9.3% coolant and 8.5% Zircaloy-2. The type of coolant in this study is either natural Li or Na.

In blanket #1, natural Li is used as coolant in the front zone (10 cm) and in the fuel zone. Enriched lithium (50% Li-6) is used in the lithium absorbing zone (zone 10). The UBR and TBR are 0.71 and 1.1, respectively; when using Na as the coolant in the front and fuel zones (blanket #2), the UBR increases to 1.34 and the TBR dropped to 0.097. Although the utilization of the D-T neutron in fuel and tritium production is higher in blanket #1 ($0.71 + 1.1 = 1.81$) than in blanket #2 (1.43), the UBR is noticeably higher in blanket #2.

The 25 locations reserved for control rods were filled with natural lithium in blanket case #3, then 50% enriched lithium and Na as the coolant (blanket #4). The competition between Li and Th to absorb neutrons in the fuel zone tends to decrease the UBR (to 1.14) and to increase the TBR (to 0.38) in blanket #3. The corresponding values in blanket #4 are UBR = 0.9 and TBR = 0.67. One should notice that TBR + UBR is almost the same for blanket #3 and 4. This shows that increasing TBR is at the expense of decreasing UBR.

CASE NUMBER

Blanket	#1	#2	#3	#4	#5	#6	#7	#8	#9	#10	#11	#12	#13
Zone 1, 2	Zone 1 Point Source Within 0.5 cm Radius Zone 2 Void 499.5 cm Thickness												
Zone 3	82.2% Be 9.3% Nat. Li Coolant 9.5% Zirc-2 (10 cm)	As #1 but with Na Coolant		As #2 (0 cm)	As #2 (5 cm)	As #2 (15 cm)	100% Pb4-Li Mat. Li (10 cm)	As #2 Pb Re- places Be (5 cm)	As #9 (10 cm)	As #9 (15 cm)	As #9 (20 cm)	As #10	
Zone 4	(0 cm)												
Zone 5, 7	100 % SS (0.5 cm)												
Zone 6	30.3% ThO ₂ 9.2% Zirc-2 59.2% Nat. Li Coolant 1.3% Void (21.4 cm)	As #1 but with Na Coolant	30.3% ThO ₂ 3.8% Nat. Li 55.4% Na Coolant 9.2% Zirc-2 7.3% Void (21.4 cm)	As #3 but Li Is 50% Li6				As #1 but with Pb4Li Coolant. Nat. Li Is Used	As #2				
Zone 8	(0 cm)												
Zone 9	Pb+C Mixture 66.6% C 33.4% Pb (60 cm)												
Zone 10	95% Li (50% Li6) 5% SS (10 cm)												
Th(n,γ)UBR	0.7132	1.3357	1.1364	0.8970	0.7492	0.9040	0.8230	1.1259	0.8589	0.9567	1.0116	1.0392	0.9338
TBR	0.0998	0.0968	0.3797	0.6703	0.5226	0.5353	0.8003	0.5029	0.6152	0.5946	0.5734	0.5487	0.6254
Th(v _{0f})	0.1158	0.1185	0.1184	0.1183	0.1909	0.1527	0.0899	0.0704	0.1218	0.0799	0.0520	0.0338	0.0799
	0.1159	1.9818											

Table 2

Neutronic Results for Different Blankets

The effect of the Be front zone thickness was studied via the cases, blanket #5 (0 cm front zone), blanket #6 (5 cm), blanket #4 (10 cm) and blanket #7 (15 cm). In these blankets the coolant in the front zone and fuel zone is Na and the 25 locations reserved for control rods were filled with 50% Li-6 enriched lithium. The back lithium zone was kept at 10 cm with 50% Li-6 enriched lithium. Table 3 gives the reaction rates for blanket cases #6, #4 and #7, respectively. The first 7 rows of this table show the reaction rates which lead to neutron multiplication, in particular the $(n,2n)$ reaction for the structural materials and $(n,2n)$, $(n,3n) \times 2$ and $(n, \nu \sigma_f)$ reactions for Th. Rows 8 to 17 give the absorption rate in the entire blanket while rows 18 to 21 give the reaction rates for breeding U-233 and tritium. The neutron multiplication and absorption rates in the fuel and structural materials as a function of the Be zone thickness are shown in Figure 4. The tritium production rate and the U-233 breeding rate are shown in Figure 5. For a 5 cm Be front zone, the main source of neutron multiplication comes from the $(n,2n)$, $(n,3n)$ and fast fission reactions in Th. However, there is noticeable neutron multiplication from $(n,2n)$ in Be. As the thickness of the Be zone increases, the $(n,2n)$ reaction rate in Be increases and overrides the neutron multiplication due to Th at about a 6 cm Be zone thickness. Further increase of this thickness results in larger neutron multiplication in Be. However, an increase in the Be zone thickness leads to a softer neutron spectrum throughout the blanket. This leads to a decreased rate of fission, $(n,2n)$, and $(n,3n)$ reactions in Th.

The main source of neutron absorption is due to Th (n, abs) and $\text{Li}^6(n, \text{abs})$ as shown in Fig. 4, Fig. 5, and Table 3. The

Table 3
Reaction Rates of Blanket #6, #4 and #7 per D-T Neutron

Type	Reaction	Blanket #6 (5 cm)	Blanket #4 (10 cm)	Blanket #7 (15 cm)
Source	Th (n,2n) + (n,3n) + (n,ν _{of})	0.3645	0.2775	0.2077
	Be (n,2n)	0.2848	0.5585	0.7876
	Structure (n,2n)	0.0957	0.0958	0.0961
	Na (n,2n)	0.0035	0.0027	0.0022
	Pb (n,2n)	0.0643	0.0471	0.0344
	D-T neutron SUM	1.0 1.8129	1.0 1.9815	1.0 2.1279
Sink	Th (n,abs)	0.9481	0.9319	0.8501
	Be (n,abs)	0.0347	0.0732	0.1175
	Structure (n,abs)	0.0918	0.1399	0.2032
	Na (n,abs)	0.0519	0.0612	0.0928
	⁶ Li (n,abs)	0.5202	0.6477	0.7677
	⁷ Li (n,abs)	0.0001	0.0001	0.0001
	Pb + C (n,abs)	0.1251	0.0957	0.0723
	0	0.0337	0.0262	0.0199
	Leakage	0.0084	0.0064	0.0049
	SUM	1.8138	1.9825	2.1284
Breeding	Th (n,γ)	0.9040	0.8970	0.8230
	⁶ Li (n,t)α	0.5308	0.6667	0.7974
	⁷ Li (n,t)α	0.0045	0.0036	0.0078
	Li (n,t)	0.5353	0.6703	0.8003

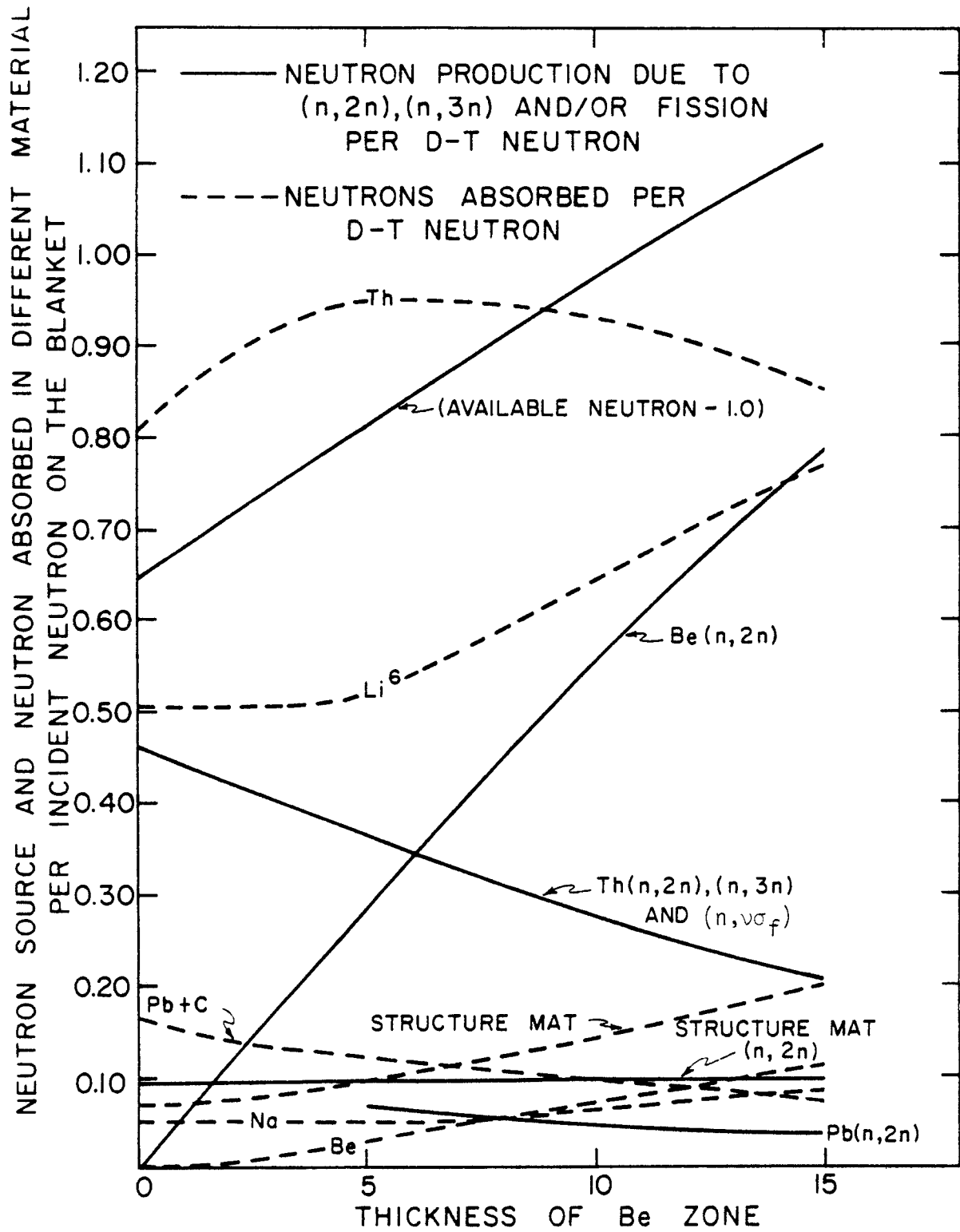


Fig. 4 NEUTRON SOURCES AND SINKS AS FUNCTION OF Be FRONT ZONE THICKNESS

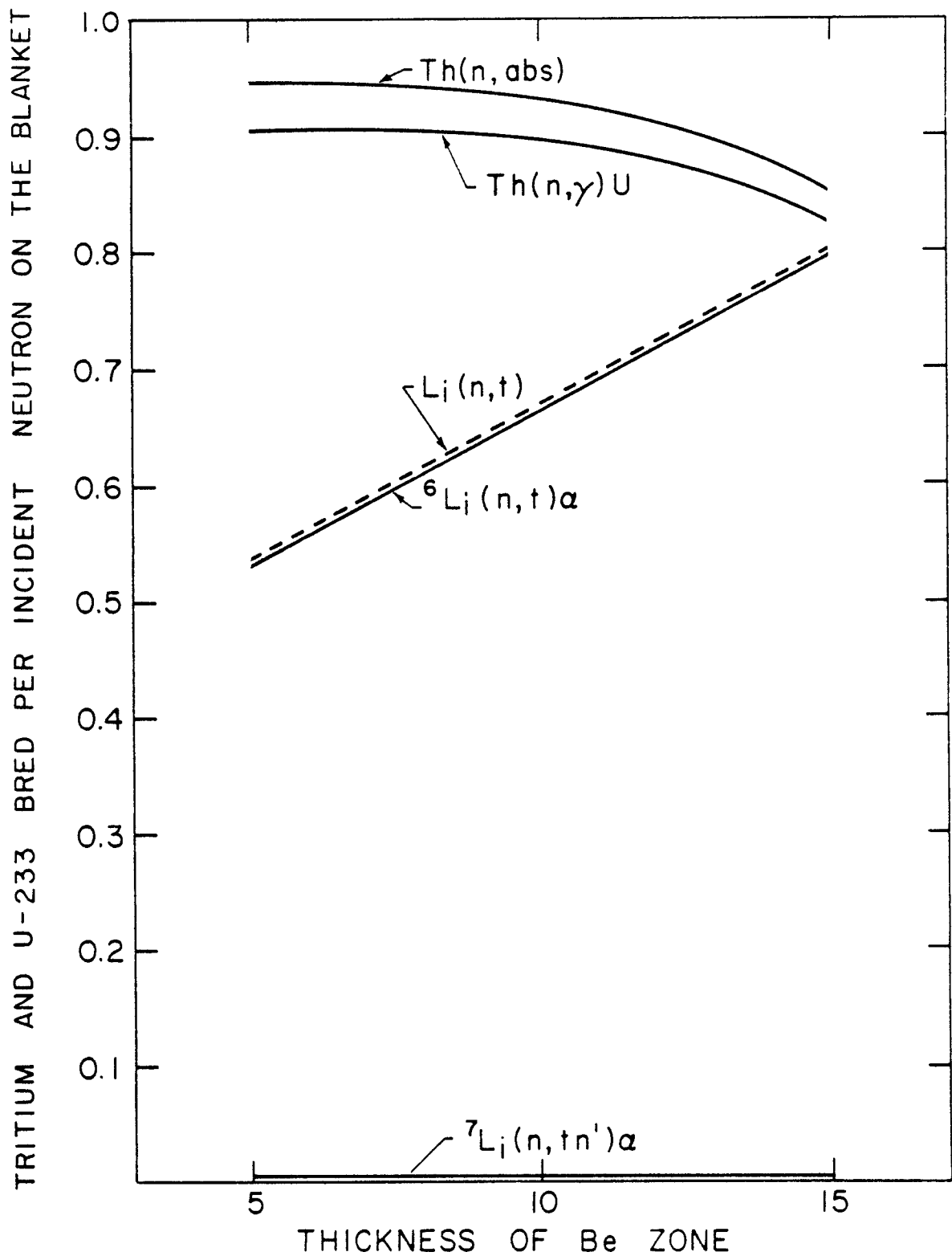
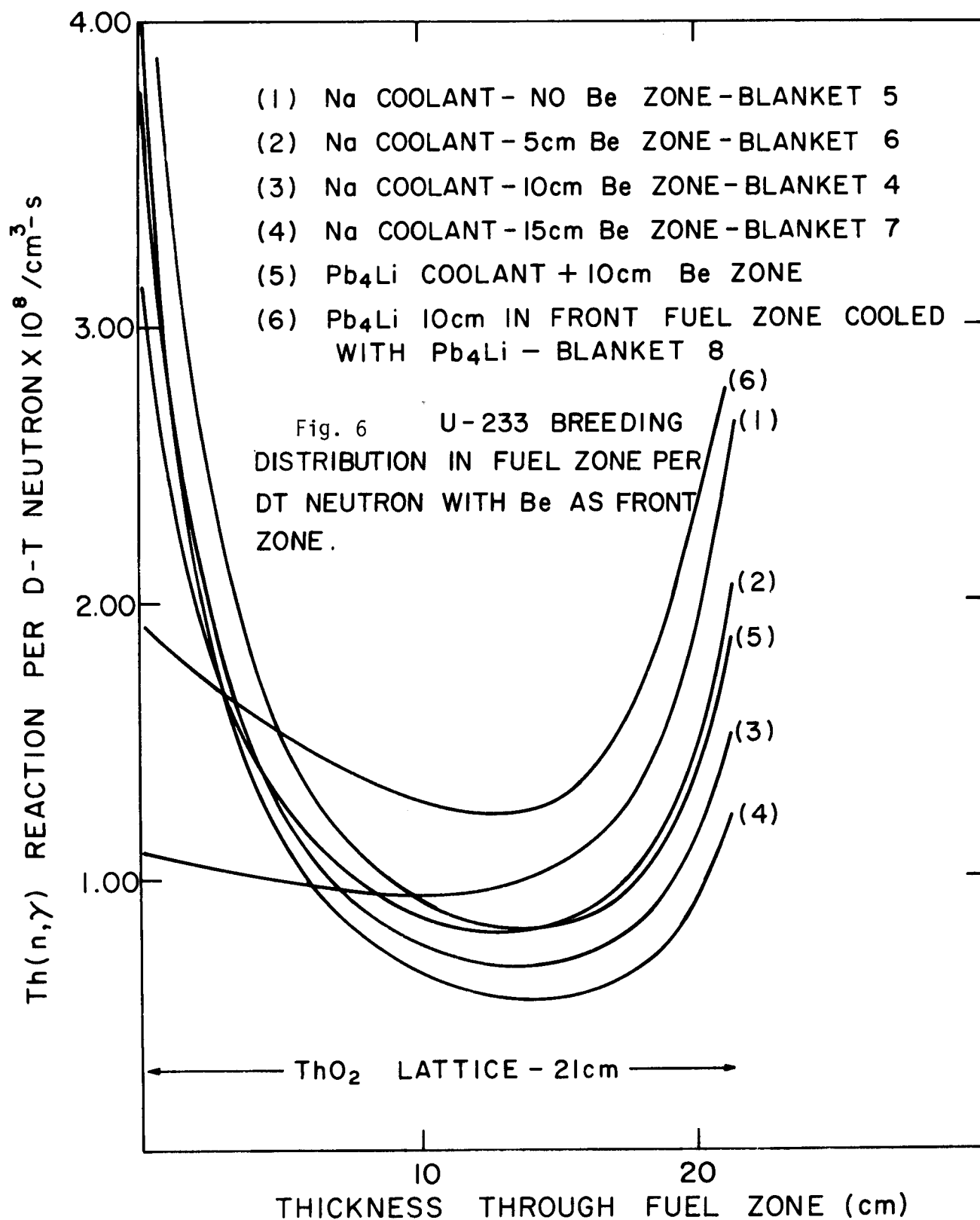


Fig. 5 Tritium and U-233 Breeding Rates as Function of Be Front Zone Thickness per D-T Neutron

percentage of neutrons absorbed in Th compared to the total number of neutrons available is 52.3%, 47%, and 40% for the 5 cm, 10 cm and 15 cm Be zone thickness cases, respectively. For Li^6 , the corresponding values are 28.6%, 32.7% and 36%, respectively. The main sources of neutron production are the $\text{Th}(n,2n)$, $\text{Th}(n,3n)$, $\text{Th}(n,\nu\sigma_f)$ and $\text{Be}(n,2n)$ reactions. The percentage of neutrons from Th compared to the total neutrons available in the blanket are 20%, 14% and 9.8% for 5, 10 and 15 cm Be front zone cases, respectively. The corresponding values for the $\text{Be}(n,2n)$ reaction are 15.7%, 28.2% and 37%, respectively. This shows the effectiveness of Be as a front zone neutron multiplying material. In going from 0 cm to 5 cm Be front zone thickness, the UBR increases from 0.75 to 0.9. It then slightly decreases as the Be zone thickness increases further. In contrast, TBR increases monotonically as the front zone thickness increases. This again is due to the increasingly softer spectrum produced by neutron moderation in Be which permits the $\text{Li}^6(n,t)\alpha$ reaction to dominate capture in thorium. The optimum thickness for the Be front zone is about 10 cm. In this case, UBR is 0.9 and TBR is 0.67. The latter value meets the requirement that TBR in the spherical mock-up calculations be ~ 0.6 . The end caps in the final design make up the remainder.

The constraint of uniform U-233 distribution throughout the fuel assembly is not met in this series of blankets. The $\text{Th}(n,\gamma)$ reaction rate per D-T neutron throughout the fuel zone is shown in Fig. 6 for blankets #4, #5, #6 and #7, respectively. The reaction rate first decreases and then increases again due to the neutrons from the reflector zone. As the thickness of the Be zone increases, the curves tend to increase in front and decrease in the back. The minimum occurs even closer to the back edge. In general, the fuel zone in this series is self-shielded to fissile fuel production.



When Pb_4Li eutectic replaced the Na coolant of blanket #1, the UBR and TBR become 1.1 and 0.68, respectively. However, the $\text{Th}(n,\gamma)$ curve is still steep both in the front and the back edges of the fuel zone (see Fig. 6, curve 5). When 100% Pb_4Li is used as a front zone neutron multiplier (blanket #8) and Pb_4Li is the coolant in the fuel zone, the steepness of the U-233 production rate near the front edge of the fuel zone decreases noticeably (again see Fig. 6, curve 6).

The adequate performance of blankets using Pb and Li in front of the fuel zone leads us to the second series of blankets that utilizes the Pb as a base for the front zone.

IV-3. Lead as the Neutron Multiplier

Cases 9 through 13 are blanket models with varying thicknesses of the Pb containing neutron multiplier zone (zone #3). Further, the multiplier zone is followed by 1.5 cm of nat. liquid lithium (with volume percentage of 95% Li and 5% S.S.) and the fuel zone is followed by a 6 cm zone of 95% natural Li and 5% S.S. The purpose of these zones as thermal neutron filters and tritium breeders was discussed earlier. For blanket #10, with a 10 cm Pb multiplier zone, the UBR and TBR are 0.96 and 0.6, respectively. The competition between the $\text{Th}(n,\gamma)$ and the $\text{Li}^6(n,t)\alpha$ reactions for neutron absorption does serve to flatten the $\text{Th}(n,\gamma)$ reaction rate profile in the fuel assembly.

Various reaction rates per D-T neutron for cases of 5 cm, 10 cm, 15 cm and 20 cm Pb front zone thickness are given in Table 4 and shown on Fig. 7. **These cases are for blankets #9, #10, #11, and #12, respectively. Blanket #10' is the same as blanket #10 with 50% Li-6 enriched Li in zone 4.**

Table 4. Reaction Rates of Blanket #9, #10, #10', #11, #12,
and #13 Per D-T Neutron

Blanket Parameter	#10' (10 cm)	#9 (5 cm)	#10 (10 cm)	#11 (15 cm)	#12 (20 cm)	#13 (10 cm)
Th(n, γ)	0.7886	0.8589	0.9567	1.0116	1.0392	0.9339
max/min after rotation	1.0739	1.2114	1.2694	1.3412	1.4318	1.2185
TBR(Li-6)	0.7722	0.5774	0.5707	0.5585	0.5395	0.5983
TBR(Li-7)	0.0189	0.0378	0.0239	0.0149	0.0092	0.0271
TBR (total)	0.7910	0.6152	0.5946	0.5734	0.5487	0.6254
Fraction of TBR from Zone 4	0.1434	0.1664	0.1979	0.2294	0.2674	0.1874
Fraction of TBR from Zone 8	0.7812	0.6779	0.6609	0.6392	0.6116	0.6876
Fraction of TBR from Zone 10	0.0754	0.1557	0.1412	0.1313	0.1211	0.1250
Th (n, $\nu\alpha_f$)	0.0798	0.1218	0.0799	0.0520	0.0338	0.0799
Th (n,2n)	0.0633	0.1020	0.0634	0.0390	0.0239	0.0634
Th (n,3n)x2	0.0379	0.0619	0.0379	0.0230	0.0138	0.0379
Sum Th	0.1810	0.2857	0.1812	0.1140	0.0715	0.1812
Pb(n,2n)	0.4937	0.3239	0.4938	0.6008	0.6668	0.4919
Fraction Pb(n,2n) from Zone 3	0.9514	0.8776	0.9513	0.9757	0.9868	0.9551
Fraction Pb(n,2n) from Zone 9	0.0486	0.1224	0.0487	0.0243	0.0132	0.0449
Pb(n,abs)	0.0692	0.0967	0.0976	0.1024	0.1095	0.0918
$\frac{Pb(n,abs)}{Pb(n,2n)}$	0.1401	0.2987	0.1977	0.1705	0.1642	0.1867

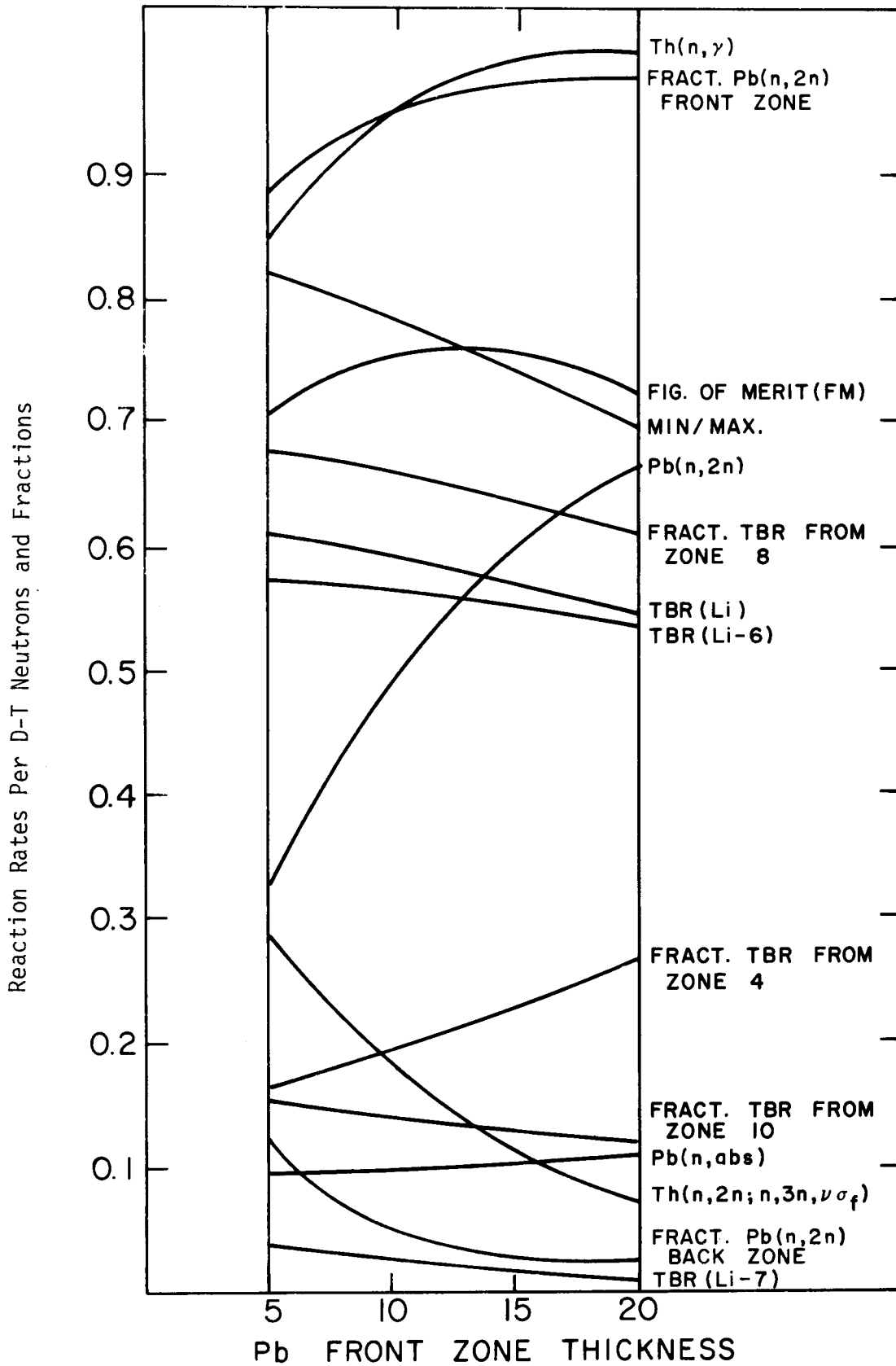


Fig. 7 THE REACTION RATES PER D-T NEUTRON
V S. Pb FRONT ZONE THICKNESS

Increasing the Pb zone thickness increases the $\text{Th}(n,\gamma)$ reaction rate but the increase is slowed when the zone thickness exceeds about 15 cm. The $\text{Li}^6(n,t)\alpha$ reaction rate steadily decreases as the front zone thickness increases. Almost all the tritium produced comes from the $\text{Li}^6(n,t)\alpha$ reaction. The fraction of tritium produced in zone 4 increases from 17% to 27% as the front thickness increases from 5 cm to 20 cm because the spectrum becomes softer. The highest fraction of tritium produced is in zone 8 (~65% for blanket #10). This fraction decreases as the front zone thickness increases. The Li back zone contributes ~14% to the total tritium produced. This fraction decreases steadily as the front zone thickness increases.

The main source of neutron multiplication is the $\text{Pb}(n,2n)$ reaction. It increases from ~0.32 to ~0.67 per D-T neutron as the front zone thickness increases from 5 cm to 20 cm. This shows the effectiveness of Pb as a front zone neutron multiplier. As expected, the fraction of $\text{Pb}(n,2n)$ reactions from the front zone is much higher than the corresponding value in the reflector zone (~95% for blanket #10) and increases as the front zone thickness increases. The absorption rate in Pb is small (0.098 for blanket #10). The value of $\text{Pb}(n,\text{abs})/\text{Pb}(n,2n)$ decreases as the front Pb zone thickness increases.

The radial profiles for the $\text{Th}(n,\gamma)$ reaction rate through the fuel zone are shown on Fig. 8. These curves are much less steep than the corresponding ones shown in Fig. 6 where Be is the neutron multiplier. To flatten the $\text{Th}(n,\gamma)$ reaction rate profile at the back edge of the fuel zone and to gain a higher value of TBR, blanket #10 is modified by increasing the Li zone thickness behind the fuel zone from 6 cm to 8 cm.

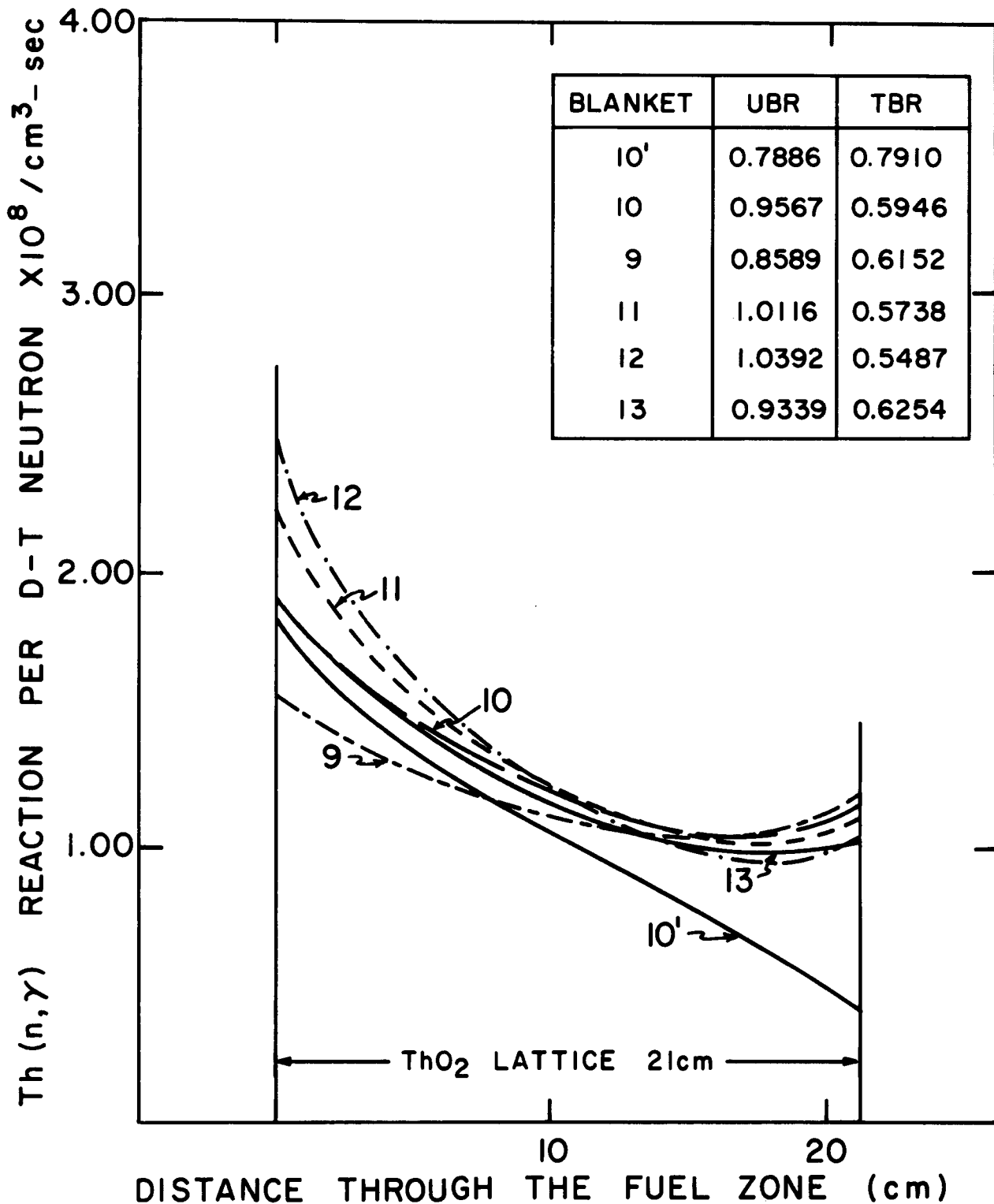


Fig. 8 U-233 BREEDING RATE DISTRIBUTION
IN FUEL ZONE PER D-T NEUTRON
WITH Pb AS THE FRONT ZONE
NEUTRON MULTIPLIER

The UBR and TBR for this modified blanket (blanket #13) are 0.94 and 0.63, respectively. The reaction rates for this blanket are given in Table 4 and the $\text{Th}(n,\gamma)$ reaction rate across the fuel zone is shown in Fig. 8.

IV-4. Optimization Criteria

From the analysis just discussed, one is motivated to use lead as the neutron multiplier in the blanket front zone since the $\text{Th}(n,\gamma)$ reaction rate profile in the fuel zone is more uniform. The spectrum in the fuel zone is harder. In addition, lead, unlike beryllium does not pose a resource availability problem. Further, for the lead based blankets, the optimized one should meet the following requirements:

- . Maximum U-233 production rate with as flat a U-233 distribution across the fuel assembly as possible.
- . TBR ~ 0.6 . Overall TBR ≥ 1.0 .

The first requirement shortens the residence time of the fuel to reach a specified enrichment. The constraint of a flat U-233 profile minimizes hot spot problems when the fuel assembly is placed directly in an LWR without an intermediate reprocessing step.

To begin the optimization search, it is assumed that the $\text{Th}(n,\gamma)$ reaction rate profile across the fuel zone does not change when the fuel assembly is rotated 180° at any time which is short enough before the bred U-233 changes the neutronics of the blanket. This assumption has been verified and is discussed in Ref. (15) which is devoted to the time behavior of the blankets studied in this report. The resultant curve, obtained by the addition of the $\text{Th}(n,\gamma)$ profile to its spatially reversed value to account for the 180° rotation, is symmetric. The resultant curve based on the blanket clean condition composition (i.e., at the beginning of life of the blanket) is taken as the base for choosing the optimized blanket in our design.

The resultant curves obtained for blankets #9, #10, #10', #11, #12 and #13 are shown in Fig. 9. The maximum-to-minimum value of these curves is given in Table 4.

According to our criteria and constraints, the optimized blanket will be the one having the smallest maximum-to-average $Th(n,\gamma)$ reaction rate, denoted by R , for its resultant curve while having a high value of UBR. Thus, the figure of merit, FM, is UBR/R and this should be a maximum. However, FM is proportional to $(UBR)^2/Th(n,\gamma)_{\max}$ since the average $Th(n,\gamma)$ reaction rate value is proportional to UBR. The FM values $\times 10^{-8}$ are given in Fig. 9.

Although blanket #12 has the highest value of FM, blanket #13 is chosen as the optimized one to gain the economic benefit of a 10 cm front zone rather than 20 cm (this is a thinner and cheaper blanket). The FM values are nearly equal in both cases. The optimized blanket #13 has TBR = 0.625 which meets the second constraint cited earlier.

V. Conclusions

An optimized blanket utilizing lead as a front zone neutron multiplier has been chosen. It has UBR and TBR of 0.94 and 0.625, respectively. This blanket has a high figure of merit value and a nearly flat U-233 production rate across the fuel zone. Carrying out a 180° fuel assembly rotation after half the residence time to reach a specified enrichment will give a symmetric U-233 distribution in the fuel assembly.

The final SOLASE-H fission-fusion laser driven hybrid reactor is based on the optimized blanket obtained from this study. This final design is given in Fig. 1.

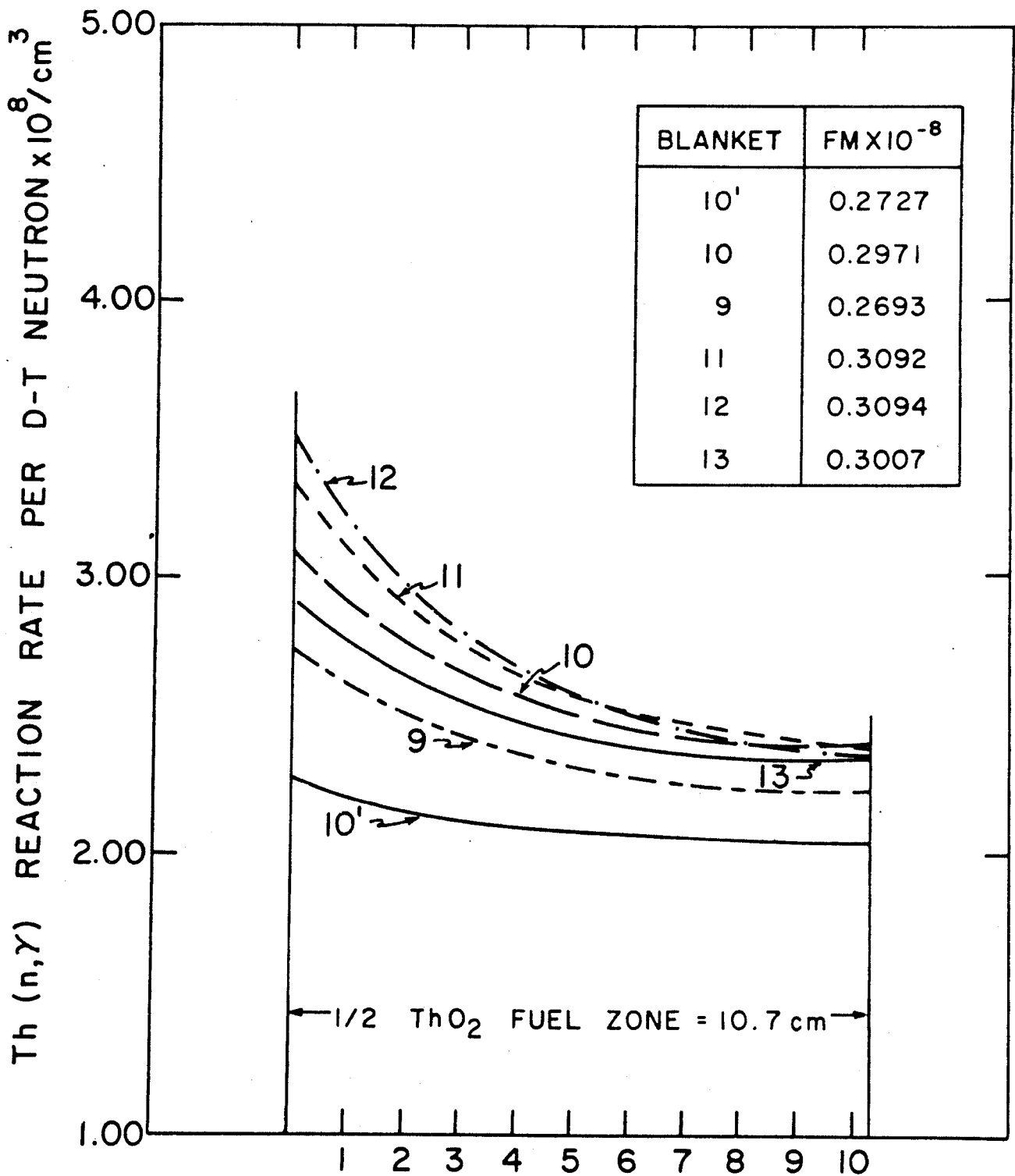


Fig. 9

U-233 BREEDING RATE DISTRIBUTION
THROUGH 1/2 OF THE FUEL ZONE
AFTER ROTATION

VI. References

1. Rose, R.P., "Status of Westinghouse Tokamak Hybrid Studies", Proceedings of the Second Fusion-Fission Energy Systems Review Meeting, Washington, D.C., Nov. 2-3 (1977), CONF-771155, Vol. I, 123 (July 1978).
2. Varljen, T.C., "New Initiatives in Tokamak Hybrid Studies", Ref. 1, 251, July (1978).
3. Tenney, F.H., "Reactor Studies of Tokamak Hybrids", Proceedings of the Second Fusion-Fission Energy Systems Review Meeting, Washington, D.C., Nov. 2-3 (1977), CONF-771155, Vol. II, 523, July (1978).
4. Allen, W.O. and Thomson, S.L., "Electron Beam Fusion-Fission Reactor Studies", Third ANS Topical Meeting on the Technology of Controlled Nuclear Fusion, May 9-11, 1978, Santa Fe, NM.
5. Bender, D.J., "Mirror Hybrid Studies", Ref. 1, 99, July (1978).
6. Lee, J.D., Bender, D.J., Moir, R.W., and Schultz, K.K., "Mirror Hybrids - A Status Report", Proc. Second Topical Meeting on the Technology of Controlled Nuclear Fusion, Washington 1976, CONF-760935-P2, pg. 689.
7. Maniscalco, J.A. and Hansen, L.F., "Present Status of Laser Driven Fusion-Fission Energy Systems", Ref. 1, Pg. 145, July (1978). Also, "New Initiatives in Laser Driven Fusion-Fission Energy Systems", Ref. 1, pg. 277, July (1978).
8. Conn, R.W., Moses, G.A., and Abdel-Khalik, S.I., "Notes on Fusion Hybrid Reactors", UWFD-240, Fusion Research Program, The University of Wisconsin, April (1978).
9. "Proceedings US-USSR Symposium on Fusion-Fission Reactors", CONF-760733, July (1976). This reference includes different hybrid designs. Also see CONF-771155, Vol. I & II, July (1978).
10. Feiveson, H.A. and Taylor, T.B., "Alternative Strategies for International Control of Nuclear Power", Report Prepared for the 1980's Project of Council on Foreign Relations, Oct. (1976).
11. Feiveson, H.A. and Taylor, T.B., Bull. of Atomic Sci. 32, 14 (1976).
12. Bethe, H.A., "The Fusion Hybrid", Nuclear News, pg. 41-44, May (1978).
13. Moses, G.A., Conn, R.W., and Abdel-Khalik, S.I., "Laser Fusion Hybrids- Technical, Economic and Proliferation Considerations", UWFD-272, Fusion Research Program, The University of Wisconsin, Nov. (1978).
14. Conn, R.W., et al., "SOLASE-H, A Laser Fusion Hybrid Reactor Study", UWFD-274, Nuclear Engineering Department, The University of Wisconsin (1978). Also, Trans. Amer. Nucl. Soc., 27, 58 (1978).

15. Youssef, M.Z., Conn, R.W., and Moses, G., "Burnup Calculations for the Laser Driven Fusion-Fission Factory, SOLASE-H", UWFDM-264, Fusion Research Program, The University of Wisconsin, October (1978).
16. K.R. Schultz, R.H. Brogli, G.R. Hopkins, M. Jonzen, and G.W. Shirley, "A U-233 Fusion-Fission Power System Without Reprocessing", A preliminary report, General Atomic GA-A14635, UC-code, Sept. (1977).
17. S.F. Su, G.L. Woodruff, N.J. McCormick, "A High-Gain Fusion-Fission Reactor for Producing U-233", University of Washington, Nuc. Technology, Vol. 29, p. 392, June (1976).
18. A.C. Cook and J.A. Maniscalco, "U-233 Breeding and Neutron Multiplying Blankets for Fusion Reactors", Lawrence Livermore Laboratories (LLL), Reprint UCRL-77284, Sept. (1975).
19. J.A. Maniscalco, "A Conceptual Design Study for Laser Fusion Hybrid", Reprint UCRL-78682, Sept. (1976).
20. J.A. Maniscalco, L.F. Hansen, and W.O. Allen, "Scoping Studies of U-233 Breeding Fusion Fission Hybrid", (LLL) Reprint UCRL-80585, May (1978).
21. W.W. Engle, Jr., "A User's Manual for ANISN", RISC-CCC-82, Oak Ridge National Lab. (1967).
22. R.Q. Wright and R.W. Rossin, "DLC-2D/100G Neutron Transport Cross Section Data Generated by SUPERTOG from ENDF/B3", RISC data package DLC-2, July (1973).
23. R.Q. Wright, et al., "SUPERTOG: A Program to Calculate Fine Group Constants and Pn Scattering Matrices from ENDF/B", ORNL-TM-2679 (1969).
24. Duderstadt, J.J., "Nuclear Reactor Analysis", John Wiley & Sons, Inc., pg. 635 (1976).